Scattering by an elastic cylinder embedded in a fluid sediment. Generalized Method of Images (GMI) approach.

Arnaud Coatanhay [a] Jean-Marc Conoir [b]

[a] *E^3I^2 Laboratoire d'Extraction et Exploitation de l'Information en Environnements Incertains, CNRS EA 3876 ENSIETA, Rue Francois Verny, 29806 Brest (France).*
Arnaud.Coatanhay@ensieta.fr

[b] *LAUE-Laboratoire d'Acoustique Ultrasonore et d'Électronique, CNRS UMR 6068 Université du Havre, Place R. Schuman, 76610 Le Havre (France).*

Abstract

An original method is presented for calculating the scattered acoustic field due to a plane wave incident upon an infinitely long elastic cylinder embedded in a sedimentary medium. The sedimentary medium is an half space domain bounded by a fluid. The cylinder is parallel to the plane interface between the sedimentary and fluid media.

First, in order to estimate the scattering by a cylinder close to a plane interface, an analytical model that generalizes the method of images, restricted to rigid and soft interfaces, is described. The validity and the accuracy of this new approach are analyzed.

Under some assumptions, the transmission, from the sediment to the surrounding fluid, of the acoustic field scattered by the embedded cylinder is evaluated. then, the detection from the fluid medium of the buried elastic cylinder resonances is treated.

Key words: Acoustic scattering; Embedded cylinder; Method of images; Plane interface

1 Introduction

In free space, the scattering by a cylindrical object is usually estimated by modal series. Theoretically, these analytic models provide an exact solution that leads to relevant physical interpretations. Insofar as the cylinder is near a plane interface, the physical problem becomes far more complex and the use of modal theories has to be considered as a debatable approach. If the plane interface is an impenetrable surface (rigid or soft), the well known method of images considers the scattered field as the scattering due to an image cylinder mirrored by the plane interface [1–4]. Note also that modal theories can be applied for studying the multiple scattering by two or more parallel cylinders [5, 6].

In bounded space, modal theories are difficult to manage and the most common methodologies usually used are finite elements, finite differences and boundary integral equation methods (BIEM) [7]. However, these methods fail to give accurate results with the increase of the frequency. For high frequences, the Geometrical Theory of Diffraction (GTD) constitutes the most appropriate method to use. Unfortunately, the ray theories do not easily apply to accurate description for complex scatterer (non standard shapes, various medium properties,...) and complex systems with strong mutual interactions.

When the cylinder is embedded in a sediment bounded by a penetrable plane interface, the scattering problem must take into account the transmission through the interface. Numerical methods and GTD are not the only available approaches. In the case of a spherical point source close to the interface, the emitted field can be expressed as an integral of plane waves of different incidence on a real domain. Assuming the reflection coefficent of the penetrable interface as known, the reflection of each plane wave can be easily determined, and then using the linearity and the principle of superposition the reflection of the point source can be calculated. This approach leads to a complex image method fully described with many reference in [8]. Unfortunately, in the case of a cylindrical point source, the corresponding integral of plane waves requires an integration path in complex space. We will see that this change induces problems of divergence in the modal series. In addition, in the case of an object close to the interface, the model must take into account the interaction between the object and the plane interface. Coatanhay et al. [9] recently developed a Generalized Method of Images (GMI) that can be applied to a cylinder close to a penetrable plane interfaces. The purpose of this paper is to present the GMI for estimating the acoustic field scattered by an elastic cylinder embedded in a sedimentary medium bounded by a plane interface.

In the first part, the acoustic field scattered in the sediment is investigated. For the sake of clarity, we reintroduce the Generalized Method of Images (GMI) theory that was developed in previous references [9, 10]. However, in the present paper, several changes are introduced to describe this theory in a more synthetic way. Actually, the GMI approach appears as a well adapted method to determine the mutual interaction between the cylinder and the penetrable fluid-sediment interface.

In the second part, we assume that the observer is located in the fluid medium. In this case, the main difficulty stands in the calculation of the transmitted component of the acoustic field scattered by the cylinder. Assuming quite high frequency waves, we can show that the method of steepest descent provides an asymptotic approximation of the transmitted field. Finally, the detection of the resonance frequencies of the elastic cylinder is treated.

2 Acoustic field in the sediment

In this paper, the acoustic incident field is a plane wave coming from the fluid. So, for an observer in the sediment, the plane wave transmitted from the fluid medium to the sediment can be considered as the only incident plane wave that impinges on the cylinder close to the interface, see figure 1.

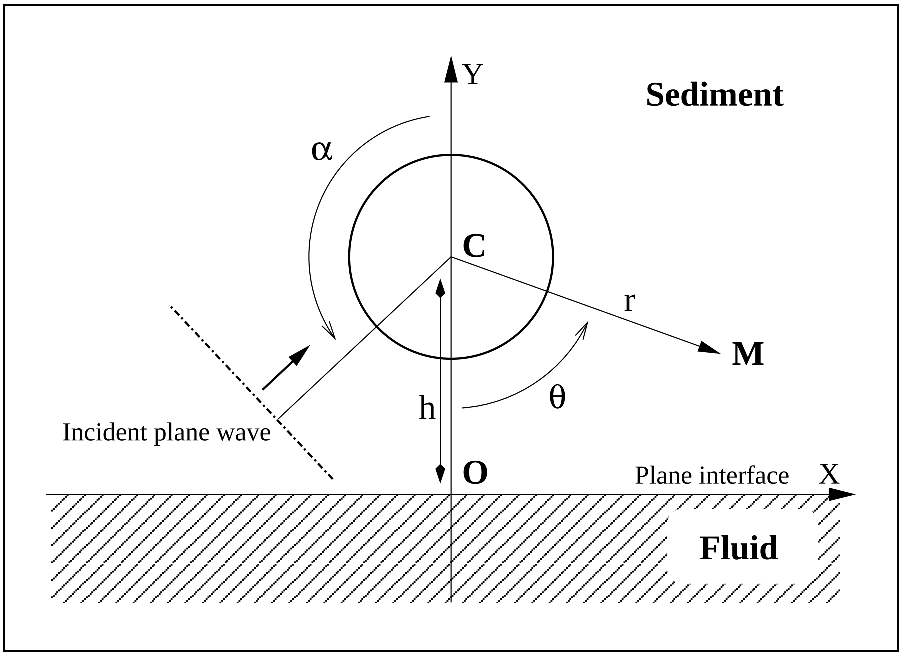

Fig. 1. *Cylinder-interface system geometry: α is the angle of incidence, C the center of the cylinder, (r, θ) the polar coordinates of the observer M, O the origin of cartesian coordinates and h the distance of the cylinder center from the interface.*

2.1 Incident wave

The direction of propagation of the incident wave is supposed to be perpendicular to the cylinder axis. As the infinite cylinder lies parallel to the interface plane. The physical problem can be reduced to a two-dimensional one.

Let C be the origin of the cylindrical coordinate system (r, θ) centered on the cylinder axis. The distance from C to the plane interface is denoted by h. In the sediment, omitting the time dependent factor $e^{-i\omega t}$, a normalized unit incident plane wave (transmitted from the fluid medium) takes the following form [11]:

$$\mathbf{p}_{incident} = e^{ik(x\sin\alpha-(y-h)\cos\alpha)} = \sum_{n=-\infty}^{+\infty} i^n e^{-in\alpha} J_n\left(kr\right) e^{in\theta} \tag{1}$$

where J_n are the Bessel functions, $k = \omega/c$ is the wave number and c is the speed of sound in the sediment.

In the fluid medium, the wave number and the sound speed are respectively denoted as $k_1 = \omega/c_1$ and c_1. In addition, we need to introduce the image of the cylinder center C_s mirrored by the plane interface that lies below the plane interface. This image point is the center of a second cylindrical coordinate system (r_s, θ_s), where the s index stands for symmetric (with regard to the plane interface).

The plane interface is acoustically characterized by the reflection coefficient of plane waves [12–15]. Letting $R\left(\alpha\right)$ be the reflection coefficient depending on the angle α, the reflected plane wave may be written as

$$\mathbf{p}_{reflected} = R\left(\alpha\right) e^{ik(x\sin\alpha+(y+h)\cos\alpha)} \tag{2}$$

The reflection coefficient $R\left(\alpha\right)$ is not only important to determine this reflected wave, but also must be considered as a fundamental parameter of the cylinder-interface scattering problem because of the interferences between the cylinder and the plane interface. The knowledge of the explicit expression of $R\left(\alpha\right)$ is not required for the mathematical expressions developed in the theoretical parts of this paper. In fact $R\left(\alpha\right)$ is only assumed to be known in this chapter.

Finally, according to the α value, the cylinder is struck either by one or two plane waves. But, in any case, the incident plane wave or the sum of the two plane waves can be considered as a single incident wave called $\mathbf{p}_{inc}$ expressed as a modal series [11]

$$\mathbf{p}_{inc} = \sum_{n=-\infty}^{+\infty} \xi_n^{(\alpha)} J_n\left(kr\right) e^{in\theta} \tag{3}$$

with

$$\xi_n^{(\alpha)} = \begin{cases} i^n \left[e^{-in\alpha} + R\left(\alpha\right) e^{ikd\cos\alpha} e^{-in(\pi-\alpha)}\right] & if \;\; |\alpha| < \pi/2 \\ i^n e^{-in\alpha} & if \;\; |\alpha| > \pi/2 \end{cases} \tag{4}$$

where $d = 2h$ is the distance between C_s and C.

Let $\xi_n^{(\alpha)}$ and $Rg\Psi_n$ be the components of the vectors $\vec{\xi}^{(\alpha)}$ and $Rg\vec{\Psi}$ with

$$Rg\Psi_n = J_n\left(kr\right)e^{in\theta} \tag{5}$$

As in electromagnetic scattering (see [16]), Rg stands for regular, in relation with the regularity of the J_n Bessel function at $r = 0$. With this usual notation, the equation (3) can always be written as

$$\mathbf{p}_{inc} = \left\langle \vec{\xi}^{(\alpha)}, Rg\vec{\Psi} \right\rangle \tag{6}$$

where $\langle \ , \ \rangle$ denotes the usual non-Hermitian product defined as

$$\left\langle \vec{a}, \vec{b} \right\rangle = \sum_{n=-\infty}^{+\infty} a_n b_n \tag{7}$$

with a_n and b_n the components of vectors $\vec{a}$ and $\vec{b}$.

For the sake of simplicity, the other modal series will be expressed in the algebraic form using the non-Hermitian product defined in equation (7).

2.2 Cylinder transition matrix

In the same way, the influence of the plane interface is characterized by a reflection coefficient, the scattering by the cylinder is determined by a linear operator denoted by $\mathbf{T}$.

As a matter of fact, any incident waves $\mathbf{p}_i$ can be written

$$\mathbf{p}_i = \sum_{n=-\infty}^{+\infty} \xi_n Rg\Psi_n = \left\langle \vec{\xi}, Rg\vec{\Psi} \right\rangle \tag{8}$$

where $\vec{\xi}$ is a vector which does not depend on the (r, θ) coordinates. It follows that the scattering by the cylinder can be expressed as [17–20]:

$$\mathbf{p}_s = \left\langle \vec{\xi}, \mathbf{T} \cdot \vec{\Psi} \right\rangle \tag{9}$$

where the Ψ_n components of $\vec{\Psi}$ the vector are the outgoing cylindrical waves defined by

$$\Psi_n = H_n^{(1)}\left(kr\right)e^{in\theta} \tag{10}$$

$H_n^{(1)}$ being the Hankel functions of the first kind (the outgoing cylindrical waves satisfy the Sommerfeld far field boundary conditions [11]). In the field of the Resonance Scattering Theory (R.S.T.) [20], the operator $\mathbf{T}$ is often called the transition matrix [21].

For circular cross section cylinder, the $\mathbf{T}$ operator is a diagonal operator, and the eigenvalues T_n $(-\infty < n < +\infty)$ are known as the modal scattering amplitudes:

$$\mathbf{p}_s = \left\langle \vec{\xi}, \mathbf{T} \cdot \vec{\Psi} \right\rangle = \sum_{n=-\infty}^{+\infty} \xi_n T_n \Psi_n \tag{11}$$

In the following sections, the reflection coefficient of the plane interface $R(\alpha)$ and the cylinder $\mathbf{T}$ matrix are supposed to be known [21]. Now, the key point is to model the interaction between the cylinder and the interface.

2.3 Reflection of a cylindrical wave

The first step to model the interaction between the cylinder and the interface is to analyze the reflection by the interface of a cylindrical wave. Applying the superposition principle, this study can be restricted to the reflection of an elementary outgoing cylindrical wave Ψ_n where n is a given mode of vibration. This study relies on the fact that the Ψ_n can be expanded as plane wave spectrum.

Indeed, the Hankel function of the first kind of order n can be written as [22]

$$H_n^{(1)}(kr) = \frac{1}{\pi} \int\limits_{W_0} e^{ikr\cos\omega} e^{in(\omega - \pi/2)}\, d\omega \tag{12}$$

where the W_0 integration path is from $W_0^s + i\infty$ with $-\pi < W_0^s < 0$ to $W_0^f - i\infty$ with $0 < W_0^f < +\pi$. According to Sommerfeld [23], by introducing the new variable θ_k as follows

$$\omega = \theta_k - \theta \tag{13}$$

the above integral can be written as

$$\Psi_n = H_n^{(1)}(kr)\, e^{in\theta} = \frac{1}{\pi} \int\limits_{W} e^{ik(x\sin\theta_k - (y-h)\cos\theta_k)} e^{in(\theta_k - \pi/2)}\, d\theta_k \tag{14}$$

where W is the Sommerfeld contour starting from $-\pi/2 + i\infty$ and ending at $\pi/2 - i\infty$ (see figure 2).

From physical point of view, θ_k represents the incident angle of a plane wave (θ_k is similar to α defined in equation (1)). It is noteworthy that equation (14) is the expression of the outgoing cylindrical wave Ψ_n in term of plane waves. Consequently, using the superposition principle of waves [15], the reflection of Ψ_n is given by

$$\Psi_{R,n} = \frac{1}{\pi} \int\limits_{W} R(\theta_k)\, e^{ik(x\sin\theta_k + (y+h)\cos\theta_k)} e^{in(\theta_k - \pi/2)}\, d\theta_k \tag{15}$$

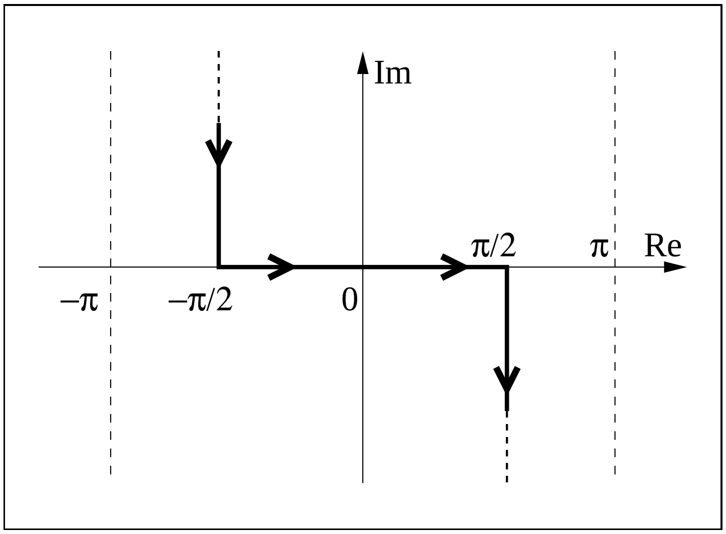

Fig. 2. *Sommerfeld path of integration.*

The equation (15) provides a usefull expression of the reflected cylindrical wave. Nevertheless, a modal series expression is required for our approach. In order to obtain this modal series, the reflection coefficient $R(\theta_k)$ is expanded as a Fourier series in θ_k:

$$R(\theta_k) = \sum_{q=-\infty}^{+\infty} R_q \cdot e^{iq\theta_k} \tag{16}$$

Once this Fourier series introduced into equation (15), we obtain

$$\Psi_{R,n} = \sum_{q=-\infty}^{+\infty} R_q \cdot i^q \cdot \left[\frac{1}{\pi} \int_W e^{ik(x\sin\theta_k + (y+h)\cos\theta_k)} e^{i(n+q)(\theta_k - \pi/2)}\, d\theta_k \right] \tag{17}$$

Then, with the use of this following expression

$$\Psi_n^{(s)} = H_n^1(kr_s)\, e^{in\theta_s} = \frac{1}{\pi} \int_W e^{ik(x\sin\theta_k + (y+h)\cos\theta_k)} e^{in(\theta_k - \pi/2)}\, d\theta_k \tag{18}$$

of the outgoing cylindrical waves coming from the image point C_s, we get:

$$\Psi_{R,n} = \sum_{m=-\infty}^{+\infty} R_{m-n} \cdot i^{m-n} \cdot \Psi_m^{(s)} \tag{19}$$

with $m = q + n$. Note that the mathematical problems related to the series covergence will be pointed out later.

By this way, we can define a reflection operator $\mathbf{R}$ with the components R_{mn} given by:

$$R_{mn} = i^{m-n} R_{m-n} \tag{20}$$

To be clearer, the reflection operator $\mathbf{R}$ looks like :

$$\mathbf{R} = \begin{pmatrix} \ddots & -iR_{-1} & -R_{-2} & iR_{-3} & \ddots \\ iR_1 & R_0 & -iR_{-1} & -R_{-2} & iR_{-3} \\ -R_2 & iR_1 & R_0 & -iR_{-1} & -R_{-2} \\ -iR_3 & -R_2 & iR_1 & R_0 & -iR_{-1} \\ \ddots & -iR_3 & -R_2 & iR_1 & \ddots \end{pmatrix} \tag{21}$$

In a formal way, letting $\Psi_{R,n}$ and $\Psi_m^{(s)}$ be the components of the vectors $\vec{\Psi}_R$ and $\vec{\Psi}^{(s)}$, the equation (19) takes the following algebraic expression:

$$\vec{\Psi}_R = \mathbf{R} \cdot \vec{\Psi}^{(s)} \tag{22}$$

In the case of rigid and soft interfaces, $R(\theta_k) = \pm 1$ respectively, so that equation (22) is reduced to

$$\vec{\Psi}_R = \pm \vec{\Psi}^{(s)} \tag{23}$$

as required by the method of images.

2.4 Elementary scattering by the cylinder

The second step to analyze the mutual interaction between the cylinder and the interface is to model the scattering by the cylinder of the cylindrical wave $\Psi_n^{(s)}$ coming from the point C_s. This problem can be solved with the use of the Graf theorem [22] from which the following relation is obtained:

$$\Psi_n^{(s)} = \sum_{m=-\infty}^{+\infty} H_{m+n}^{(1)}(kd)\, Rg\Psi_m \tag{24}$$

So, introducing the Graf operator - denoted by $\mathbf{G}$ - whose components G_{nm} are defined as

$$G_{nm} = H_{m+n}^{(1)}(kd) \tag{25}$$

equation (24) takes the vectorial form

$$\vec{\Psi}^{(s)} = \mathbf{G} \cdot Rg\vec{\Psi} \tag{26}$$

The Graf linear operator $\mathbf{G}$ looks like:

$$\mathbf{G} = \begin{pmatrix} \ddots & H_{-3}^{(1)}(kd) & H_{-2}^{(1)}(kd) & H_{-1}^{(1)}(kd) & \ddots \\ H_{-3}^{(1)}(kd) & H_{-2}^{(1)}(kd) & H_{-1}^{(1)}(kd) & H_{0}^{(1)}(kd) & H_{1}^{(1)}(kd) \\ H_{-2}^{(1)}(kd) & H_{-1}^{(1)}(kd) & H_{0}^{(1)}(kd) & H_{1}^{(1)}(kd) & H_{2}^{(1)}(kd) \\ H_{-1}^{(1)}(kd) & H_{0}^{(1)}(kd) & H_{1}^{(1)}(kd) & H_{2}^{(1)}(kd) & H_{3}^{(1)}(kd) \\ \ddots & H_{1}^{(1)}(kd) & H_{2}^{(1)}(kd) & H_{3}^{(1)}(kd) & \ddots \end{pmatrix} \quad (27)$$

Finally, it follows that the $\Psi_n^{(s)}$ elementary waves induces a wave scattered by the cylinder denoted as $\Psi_{S,n}^{(s)}$, and the equations (8,9,26) leads to the vectorial equation:

$$\vec{\Psi}_S^{(s)} = \mathbf{G} \cdot \mathbf{T} \cdot \vec{\Psi} \quad (28)$$

where $\vec{\Psi}_S^{(s)}$ is the vector formed of $\Psi_{S,n}^{(s)}$ components.

2.5 Mutual interaction

This section deals with the calculation of the acoustic field in the sediment, which is the sum of the incident wave, the waves coming from the cylinder and those coming from the interface.

Without loss of generality, the cylindrical wave coming from the cylinder can be written

$$\mathbf{p}_{cyl} = \left\langle \vec{A}, \vec{\Psi} \right\rangle \quad (29)$$

where $\vec{A}$ is a vector to be determined. Similarly, the contribution coming from the plane interface can be expressed as

$$\mathbf{p}_{int} = \left\langle \vec{B}, \vec{\Psi}^{(s)} \right\rangle \quad (30)$$

where $\vec{B}$ is a second vector to be determined.

As $\mathbf{p}_{cyl}$ is the scattering by the cylinder of the waves coming from the interface and of the incident plane wave. Using the linear operators $\mathbf{T}$ and $\mathbf{G}$, we obtain the following equation

$$\left\langle \vec{A}, \vec{\Psi} \right\rangle = \left\langle \vec{B}, \mathbf{G} \cdot \mathbf{T} \cdot \vec{\Psi} \right\rangle + \left\langle \vec{\xi}^{(\alpha)}, \mathbf{T} \cdot \vec{\Psi} \right\rangle \quad (31)$$

$$\left\langle \vec{A}, \overline{\vec{\Psi}} \right\rangle_H = \left\langle \vec{B}, \overline{\mathbf{G} \cdot \mathbf{T} \cdot \vec{\Psi}} \right\rangle_H + \left\langle \vec{\xi}^{(\alpha)}, \overline{\mathbf{T} \cdot \vec{\Psi}} \right\rangle_H \quad (32)$$

where $\langle \cdot, \cdot \rangle_H$ is the canonical hermitian scalar product and $\overline{X}$ the conjugate of the operator X. Finally, the equation (32) leads to the relation

$$\vec{A} = \overline{\mathbf{T}}^* \cdot \overline{\mathbf{G}}^* \cdot \vec{B} + \overline{\mathbf{T}}^* \cdot \vec{\xi}^{(\alpha)} \tag{33}$$

where * stands for the adjoint of the operator related to the hermitian scalar product.

Simultaneously, the acoustic field $\mathbf{p}_{int}$ can be considered as the reflection of the waves coming from the cylinder, so that the use of the linear operator $\mathbf{R}$ leads to

$$\left\langle \vec{B}, \vec{\Psi}^{(s)} \right\rangle = \left\langle \vec{A}, \mathbf{R} \cdot \vec{\Psi}^{(s)} \right\rangle \tag{34}$$

$$\vec{B} = \overline{\mathbf{R}}^* \cdot \vec{A} \tag{35}$$

The equations (33,35) yield the following linear system for the two unknowns $\vec{A}$ and $\vec{B}$

$$\begin{cases} \vec{A} = \overline{\mathbf{T}}^* \cdot \overline{\mathbf{G}}^* \cdot \vec{B} + \overline{\mathbf{T}}^* \vec{\xi}^{(\alpha)} \\ \vec{B} = \overline{\mathbf{R}}^* \cdot \vec{A} \end{cases} \tag{36}$$

The solution of equation (36) is given by

$$\begin{cases} \vec{A} = \left(\mathbf{I} - \overline{\mathbf{D}}^*\right)^{-1} \cdot \overline{\mathbf{T}}^* \cdot \vec{\xi}^{(\alpha)} \\ \vec{B} = \overline{\mathbf{R}}^* \cdot \left(\mathbf{I} - \overline{\mathbf{D}}^*\right)^{-1} \cdot \overline{\mathbf{T}}^* \cdot \vec{\xi}^{(\alpha)} \end{cases} \tag{37}$$

where $\mathbf{I}$ is the identity linear operator and $\mathbf{D} = \mathbf{R} \cdot \mathbf{G} \cdot \mathbf{T}$.

Finally, the expression of the global acoustic field $\mathbf{p}_{sediment}$ in the sediment can be explicitly determined by

$$\mathbf{p}_{sediment} = \mathbf{p}_{inc} + \mathbf{p}_{cyl} + \mathbf{p}_{int} \tag{38a}$$

so that

$$\begin{aligned} \mathbf{p}_{sediment} = & \left\langle \vec{\xi}^{(\alpha)}, Rg\vec{\Psi} \right\rangle + \left\langle \vec{\xi}^{(\alpha)}, \mathbf{T} \cdot (\mathbf{I} - \mathbf{D})^{-1} \cdot \vec{\Psi} \right\rangle \\ & + \left\langle \vec{\xi}^{(\alpha)}, \mathbf{T} \cdot (\mathbf{I} - \mathbf{D})^{-1} \cdot \mathbf{R} \cdot \vec{\Psi}^{(s)} \right\rangle \end{aligned} \tag{38b}$$

It is noteworthy that the expression of the $\mathbf{p}_{sediment}$ field can be interpreted as the result of a generalized Debye series which is the infinite sum of all the elementary interactions between the cylinder and the interface [9].

This theoretical expression may be considered as a generalization of the method of images. Indeed, when the interface is rigid or soft, the reflection $\mathbf{R}$ operator is reduced to $\mathbf{R} = \pm\mathbf{I}$ (cf. equation (23)) and $\mathbf{D} = \pm\mathbf{G} \cdot \mathbf{T}$. As a consequence, the acoustic field $\mathbf{p}_{sediment}$ (cf. equation 38b) is given by

$$\begin{aligned}\mathbf{p}_{sediment} = & \left\langle \vec{\xi}^{(\alpha)}, Rg\vec{\Psi} \right\rangle + \left\langle \vec{\xi}^{(\alpha)}, \mathbf{T} \cdot \left(\mathbf{I} - (\pm\mathbf{G} \cdot \mathbf{T})\right)^{-1} \cdot \vec{\Psi} \right\rangle \\ & \pm \left\langle \vec{\xi}^{(\alpha)}, \mathbf{T} \cdot \left(\mathbf{I} - (\pm\mathbf{G} \cdot \mathbf{T})\right)^{-1} \cdot \vec{\Psi}^{(s)} \right\rangle\end{aligned} \tag{39}$$

which is the solution deduced from the method of images [3]. This is the reason why this method was called Generalized Method of Images (GMI) [10, 24].

More recently, Fawcett developed the same idea in three dimension [25] with spherical waves from a source above the seabed. Indeed, an outgoing spherical harmonic can expressed as plane-wave spectrum

$$h_n(kr)\, P_n^m(\cos\phi) = i^{n-m} \int_0^{+\infty} \frac{hJ_m(hr) \cdot e^{i\gamma z}}{k\gamma} P_n^m\left(-\frac{\gamma}{k}\right) dh \tag{40}$$

with $\gamma = \sqrt{k^2 - h^2}$. So each elementary plane wave involves a reflected one and the spherical harmonic off the sea is given by

$$i^{n-m} \int_0^{+\infty} J_m(hr)\, e^{2i\gamma d} R(h)\, P_n^m\left(-\frac{\gamma}{k}\right) \frac{e^{i\gamma z}}{k\gamma} h\, dh$$

where $R(.)$ is the seabed reflection coefficient. Then, to introduce the image source contribution, Fawcett approximated the reflection coefficient thanks to a complex exponential series, in the same way as in equation (16), and obtained a similar theory for spherical waves. This approach is called the method of complex images by Fawcett [25].

2.6 Validity domain of GMI

At first sight, the GMI approach seems to provide an exact analytic expression, as any standard modal theory. However, GMI is based on the fact that the reflection coefficient is expanded as a Fourier series:

$$R(\theta_k) = \sum_{m=-\infty}^{+\infty} R_m e^{im\theta_k} \tag{41}$$

This expansion raises no particular problem for real angles, but it is not valid for the complex value of θ_k. In theory, the Fourier series (41) must not be used to integrate along the Sommerfeld contour. As a consequence, GMI often leads to divergent expressions and asymptotic series [26, 27]. In particular, major problems appear when the reflection coefficient is not a smooth function. For instance, the GMI approach can not be easily used in the case of fluid-solid interfaces.

However, from comparisons between numerical estimations of Green functions, Coatanhay et al. [9] showed that GMI, with optimal truncation, provides an accurate estimation of the acoustic field in the case of fluid-fluid interfaces. As far as the sediment medium can be approximated by a fluid medium, the GMI can be applied as well.

2.7 Numerical simulation

Many references have shown that a sedimentary medium could be well approximated by a fluid medium. So, for the sake of simplicity, the sediment is identified to a fluid medium in which the celerity c_1 and the density ρ_1 are respectively 1780 $m \cdot s^{-1}$ and 1320 $kg \cdot m^{-3}$. The fluid above the sediment was made up of standard water with celerity $c_2 = 1470\ m \cdot s^{-1}$ and density $\rho_2 = 1000\ kg \cdot m^{-3}$.

Generally speaking, a fluid-fluid reflection coefficient can be expressed as follows [15]:

$$R(\theta) = \frac{\rho_2/\rho_1 \cos\theta - \left[(c_1/c_2)^2 - \sin^2\theta\right]^{1/2}}{\rho_2/\rho_1 \cos\theta + \left[(c_1/c_2)^2 - \sin^2\theta\right]^{1/2}} \tag{42}$$

where the complex square root $[\cdots]^{1/2}$ is defined from the real one $\sqrt{\cdots}$

$$\left[(c_1/c_2)^2 - \sin^2\theta\right]^{1/2} = \sqrt{(c_1/c_2)^2 - \sin^2\theta} \qquad if \quad \sin\theta \leq c_1/c_2 \tag{43a}$$

$$\left[(c_1/c_2)^2 - \sin^2\theta\right]^{1/2} = i\sqrt{\sin^2\theta - (c_1/c_2)^2} \qquad if \quad \sin\theta \geq c_1/c_2 \tag{43b}$$

in order to respect the vanishing of the transmitted wave as usually required [15].

The cylinder is a circular cross section hollow tube made of aluminum alloy with the parameters density $\rho = 2790\ kg \cdot m^{-3}$, longitudinal velocity $c_L = 6557\ m \cdot s^{-1}$ and transversal velocity $c_T = 3128\ m \cdot s^{-1}$. The outer radius, denoted by a, is $a = 0.003572\ m$ and the inner radius, denoted by b, is defined as $b = 0.9\ a$.

The distance of the cylinder center from the interface is $h = 1.5\ a$, and the frequency is chosen so that the dimensionless product $ka = 20$. Figure 3 shows the acoustic field scattered by the cylinder-interface system. The ordinate and the abscissa of the observer are divided by the outer radius a to obtain dimensionless co-ordinates. The plane incident wave impinges the cylinder at a normal angle ($\alpha = 0$). Finally, to compute these 1000×1000 pixels, our algorithm requires only several minutes with a standard PC.

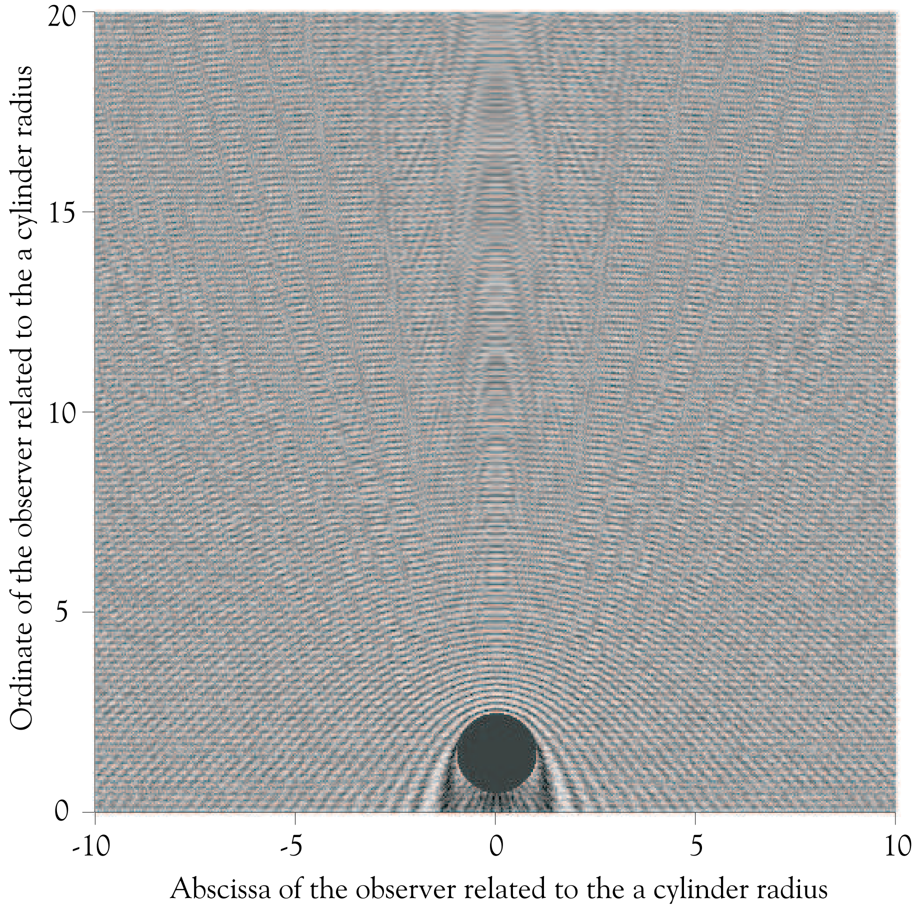

Fig. 3. *Acoustic field scattered by an elastic tube close to a plane interface.*

3 Acoustic field in the fluid medium

In the previous part, we have shown that the acoustic field scattered by a cylinder in the vicinity of a plane interface could be estimated using the GMI when the observer is in the same medium as the cylinder. Now, the cylinder is still embedded in the sedimentary medium but the observer M is supposed to be in the surrounding fluid.

As shown in figure 4 the incident wave is now a unitary plane wave $\mathbf{p}_{incflu}$ that propagates in the fluid toward the plane interface

$$\mathbf{p}_{incflu} = e^{ik_{flu}\left(-x\sin\beta_{flu}+y\cos\beta_{flu}\right)} \tag{44}$$

where β_{flu} is the angle of incidence and k_{flu} the wave number in the fluid medium. At the interface, this incident plane wave generates a reflected plane wave in the fluid and a transmitted plane wave $\mathbf{p}_{incsed}$ in the sediment. The

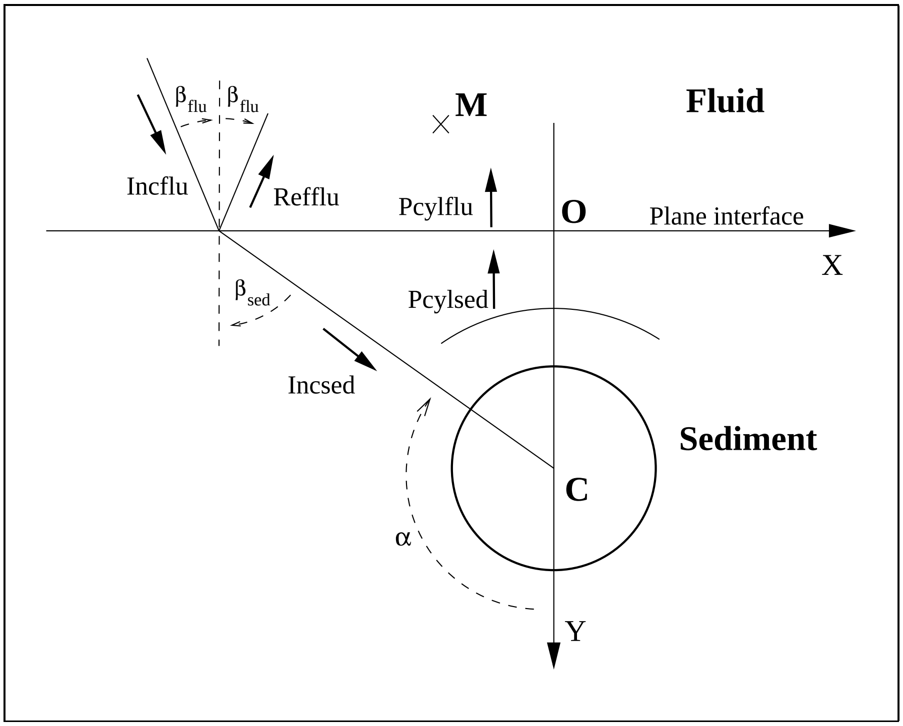

Fig. 4. *Geometrical configuration of a cylinder embedded in a sediment surrounded by a fluid.*

transmitted plane wave $\mathbf{p}_{incsed}$ is scattered by the cylinder as explain in chapter 2. This scattered waved, denoted by $\mathbf{p}_{cylsed}$ is then transmitted to the surrounding fluid to give a pressure denoted by $\mathbf{p}_{cylflu}$. Finally, the acoustic field, observed at M in the surrounding fluid, is the sum of the three acoustic waves: $\mathbf{p}_{incflu}$, $\mathbf{p}_{refflu}$ and $\mathbf{p}_{cylflu}$.

The acoustic characteristics of the both media are supposed to be known. So, with regard to the interface, the reflection coefficient in the fluid (resp. in the sediment) $R_{flu}\left(\theta\right)$ (resp. $R_{sed}\left(\theta\right)$) and transmission coefficient from the fluid to the sediment (resp. from the sediment to the fluid) $T_{flused}\left(\theta\right)$ (resp $T_{sedflu}\left(\theta\right)$) are also considered as known functions.

Applying the Snell-Descartes relation, the plane waves $\mathbf{p}_{refflu}$ and $\mathbf{p}_{incsed}$ can be expressed as

$$\mathbf{p}_{refflu} = R_{flu}\left(\beta_{flu}\right) e^{ik_{flu}\left(x\sin\beta_{flu} - y\cos\beta_{flu}\right)} \tag{45a}$$

$$\mathbf{p}_{incsed} = T_{flused}\left(\beta_{flu}\right) e^{ik_{sed}\left(x\sin\beta_{sed} + y\cos\beta_{sed}\right)} \tag{45b}$$

where k_{sed} is the wave number and β_{sed} the angle of propagation in the sediment, with

$$k_{sed}\sin\beta_{sed} = k_{flu}\sin\beta_{flu} \tag{46}$$

With regard to to the cylinder center, $\mathbf{p}_{incsed}$ can be rewritten

$$\mathbf{p}_{incsed} = T_{flused}\left(\beta_{flu}\right) e^{ik_{sed}h\cos\beta_{sed}} e^{ik_{sed}(x\sin\alpha+(y-h)\cos\alpha)} \tag{47}$$

with $\alpha = \pi - \beta_{sed}$. It follows from equations (1, 3, 4) and (8) that $\mathbf{p}_{incsed}$ can be expressed as a modal series

$$\mathbf{p}_{incsed} = \sum_{n=-\infty}^{+\infty} \xi_n^{(\alpha)} Rg\Psi_n = \left\langle \vec{\xi}^{(\alpha)}, Rg\vec{\Psi} \right\rangle \tag{48}$$

where $\xi_n^{(\alpha)} = T_{flused}\left(\beta_{flu}\right) e^{ik_{sed}h\cos\beta_{sed}} i^n e^{-in\alpha}$.

According to the GMI theory, the wave $\mathbf{p}_{cylsed}$ scattered by the cylinder is nothing else that

$$\mathbf{p}_{cylsed} = \left\langle \vec{\xi}^{(\alpha)}, \mathbf{T}\cdot(\mathbf{I}-\mathbf{D})^{-1}\cdot\vec{\Psi} \right\rangle \tag{49}$$

The last problem is now to determine how the acoustic field $\mathbf{p}_{cylsed}$ is tranmitted in the fluid. As equation (49) is a linear equation, it is sufficient to determine how an elementary cylindrical wave Ψ_n is transmitted.

3.1 Asymptotic approximations

As previously seen in equation (14), each elementary cylindrical wave Ψ_n can be expressed in the form of a plane wave spectrum

$$\begin{aligned}\Psi_n &= H_n^{(1)}(kr)\, e^{in\theta} \\ &= \frac{1}{\pi}\int_W e^{ik_{sed}\left(x\sin\theta_{k_{sed}} - (y-h)\cos\theta_{k_{sed}}\right)} e^{in\left(\theta_{k_{sed}}-\pi/2\right)}\, d\theta_{k_{sed}}\end{aligned} \tag{50}$$

The *sed* suffix used in equation (50) emphasizes the fact that the angles of propagation θ_k and the wave number $k_{sed} = \omega/c_{sed}$ are related to the propagation in the sediment.

Using the linearity and the principle of superposition the transmitted wave $\Psi_n^{(1)T}$ due to Ψ_n is given by

$$\begin{aligned}\Psi_n^{(1)T} = \frac{1}{\pi}\int_W & T_{sedflu}\left(\theta_{k_{sed}}\right) e^{ik_{sed}\left(h\cos\theta_{k_{sed}}\right)} \\ & e^{ik_{flu}\left(x\sin\theta_{k_{flu}} - y\cos\theta_{k_{flu}}\right)} e^{in\left(\theta_{k_{sed}}-\pi/2\right)}\, d\theta_{k_{sed}}\end{aligned} \tag{51}$$

where $k_{flu} = \omega/c_{flu}$ and $\theta_{k_{flu}}$ are respectively the wave number and the angle of propagation in the fluid. The angle $\theta_{k_{flu}}$ is merely deduced from the Snell-Descartes relation

$$k_{flu}\sin\theta_{k_{flu}} = k_{sed}\sin\theta_{k_{sed}} \tag{52}$$

Obviously, the general expression (51) could be estimated by using numerical methods, but the integral expressions depend on two parameters ω and n, and the global numerical estimation remains a time-consuming task.

To evaluate the expression (51) more easily, an explicit asymptotic approximation has to be performed. In fact, the k_{sed} and k_{flu} wave numbers are now supposed to be quite high. Letting

$$g_n\left(\theta_{k_{sed}}\right) = T_{sedflu}\left(\theta_{k_{sed}}\right) e^{in\left(\theta_{k_{sed}}-\pi/2\right)} \tag{53}$$

and

$$\begin{aligned} h\left(\theta_{k_{sed}}\right) &= \tfrac{k_{flu}}{k_{sed}}\left(x\sin\theta_{k_{flu}} - y\cos\theta_{k_{flu}}\right) + h\cos\theta_{k_{sed}} \\ &= \left(x\sin\theta_{k_{sed}} - y\tfrac{k_{flu}}{k_{sed}}\sqrt{1-\left(\tfrac{k_{sed}}{k_{flu}}\right)^2\sin^2\theta_{k_{sed}}}\right) + h\cos\theta_{k_{sed}} \end{aligned} \tag{54}$$

the elementary transmitted wave $\Psi_n^{(1)T}$ takes the form

$$\Psi_n^{(1)T} = \frac{1}{\pi}\int\limits_W g_n\left(\theta_{k_{sed}}\right) e^{ik_{sed}h\left(\theta_{k_{sed}}\right)}\,d\theta_{k_{sed}} \tag{55}$$

and the steepest descent method yields the following approximation of the expression (51)

$$\Psi_n^{(1)T} \simeq \begin{cases} \left(\frac{2\pi}{k_{sed}\cdot h''(\theta_{max})}\right)^{1/2} g_n\left(\theta_{max}\right) e^{i\left(k_{sed}h(\theta_{max})+\pi/4\right)} & \text{if } h''\left(\theta_{max}\right) > 0 \\ \left(\frac{2\pi}{-k_{sed}\cdot h''(\theta_{max})}\right)^{1/2} g_n\left(\theta_{max}\right) e^{i\left(k_{sed}h(\theta_{max})-\pi/4\right)} & \text{if } h''\left(\theta_{max}\right) < 0 \end{cases} \tag{56}$$

where θ_{max} is the solution of the equation $h'(\theta) = 0$.

From a physical point of view, θ_{max} represents the angle of propagation in the sediment of the ray emitted from the cylinder center that reach the observer (x, y) in the fluid. This emitted ray crosses the interface at the point $J = (x_J, 0)$, and the Snell-Descartes laws involve the relation

$$k_{sed}^2\frac{x_J^2}{x_J^2+y_c^2} = k_{flu}^2\frac{\left(x-x_J\right)^2}{\left(x-x_J\right)^2+y^2} \tag{57}$$

Then, it is easily proved that

$$\sin\theta_{max} = \frac{x_J}{\sqrt{x_J^2+y_c^2}} \tag{58}$$

and

$$\sin\theta_{max} = \frac{h}{\sqrt{x_J^2+y_c^2}} \tag{59}$$

So, for a given observer, located at (x, y)-coordinates, we can easily estimate the corresponding value θ_{max} by solving equation (57). It is noteworthy that the optimal θ_{max} angle only depends on the observer position, and is the same for every $\Psi_n^{(1)T}$ elementary functions. In that way, the approximation of $\Psi_n^{(1)T}$ is easily computed. Then, the acoustic wave coming from the cylinder and transmitted in the fluid becomes easy to determine. Finally, the GMI and the asymptotic evaluation of integrals lead to a very efficient model for calculating the acoustic field observed in the fluid.

3.2 Buried source and Green function

An efficient way to evaluate the accuracy of the asymptotic approximation we use is to compare the results obtained by this one ith those coming from an exact calculation of integrals, in the case of embedded point source in the sediment. Indeed, if we consider a buried point source, the acoustic field in the sediment that corresponds to the Green function is

$$\begin{aligned}\Psi_0 &= H_0^{(1)}\left(kr\right) \\ &= \tfrac{1}{\pi}\int\limits_W e^{ik_{sed}\left(x\sin\theta_{k_{sed}}-(y-h)\cos\theta_{k_{sed}}\right)}\,d\theta_{k_{sed}}\end{aligned} \tag{60}$$

Using equation (55), the acoustic field observed in the fluid is

$$\Psi_0^{(1)T} = \frac{1}{\pi}\int\limits_W g_0\left(\theta_{k_{sed}}\right) e^{ik_{sed}h\left(\theta_{k_{sed}}\right)}\,d\theta_{k_{sed}} \tag{61}$$

and the asymptotic approximation is given by

$$\Psi_0^{(1)T} \simeq \begin{cases} \left(\frac{2\pi}{k_{sed}\cdot h''(\theta_{max})}\right)^{1/2} g_0\left(\theta_{max}\right) e^{i\left(k_{sed}h(\theta_{max})+\pi/4\right)} & \text{if } h''\left(\theta_{max}\right) > 0 \\ \left(\frac{2\pi}{-k_{sed}\cdot h''(\theta_{max})}\right)^{1/2} g_0\left(\theta_{max}\right) e^{i\left(k_{sed}h(\theta_{max})-\pi/4\right)} & \text{if } h''\left(\theta_{max}\right) < 0 \end{cases} \tag{62}$$

For an observer in the fluid located near the plane interface, see figure 5, we can evaluate the acoustic field using the integral expression (61) and the asymptotic approximation (62). Figure 6 presents the numerical comparison between both expressions where the observer is above the sediment at an altitude half the depth of the point source. The frequency is determined so that the dimensionless product $k_{flu} \cdot r_s$ varies from 10 to 100 where r_s is the distance between the observer and the point source.

Therefore, we can notice that the asymptotic expression provides a good approximation for any observer position. Moreover, this approximation is excellent where the observer is just above the point source. In practice, this position is of the most importance to detect buried objects.

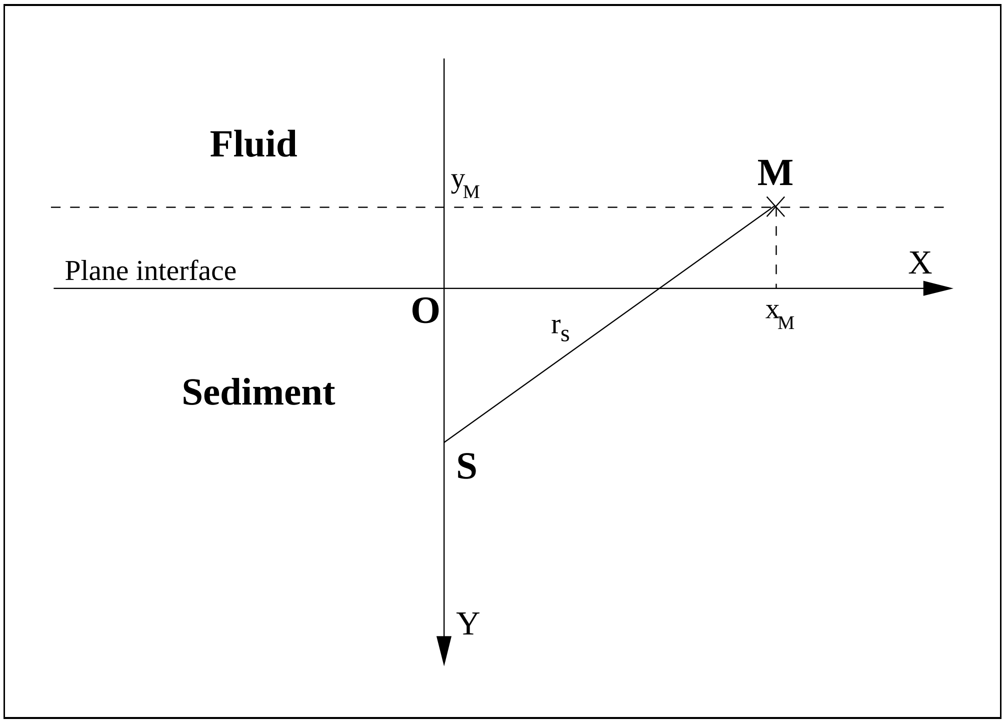

Fig. 5. *Position of the observer in the vicinity of the interface where the point source is in the sediment and the observer is in the fluid. The distance MS is denoted* r_s.

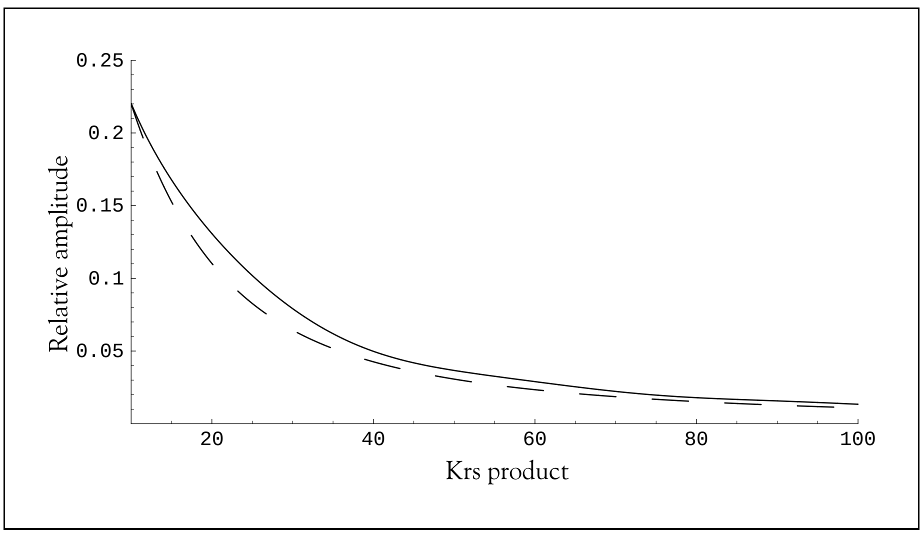

Fig. 6. *Comparison between the Green function computed with the exact integral expression (plain line) and with the asymptotic steepest descent approximation (dashed line).*

3.3 Numerical results

We now considered a buried cylindrical cross section tube made of aluminum alloy with external radius a and internal radius $0.9\,a$. The physical properties of the both media (fluid and sediment) and the aluminum alloy characteristics are the same as the previously. The distance between the tube axis and the interface is still $h = 1.5\,a$.

Figure 7 shows the amplitude of the acoustic field received by the observer in the fluid located at the coordinates $(x = 0, y = -6\,a)$, when the incident plane wave is normally incident on the interface. The product $k_{sed} \cdot a$ varies from 10 to 40. Roughly speaking, figure 7 mainly points out the interference phenomenon between the incident wave, the wave reflected by the interface and the specular wave reflected by the embedded cylinder.

This interference phenomenon depends on the geometrical configuration only. In fact, it has been verified that the interferences are governed by two characeristic distances. The one between the observer and the interface and the one between the interface and the top of the tube appear to be the most relevant parameters. In such a case, the identification of the cylinder properties seems to be an arduous challenge.

More precisely, it may be noted from figure 7 that the detection of the elastic cylinder resonances is very complicated. In order to point out these resonances we first have to remove the interface phenomenon which is the predominent phenomenon. To this end, a way consists computing the acoustic field received when the elastic is replaced by a rigid one and to sustract this field from the one obtained with the elastic cylinder. Indeed, a rigid cylinder do not resonate and the specularly reflected waves by rigid and elastc cylinders are almost the same. This is the reason why it is expected that the resonances are still detectable while the interferences vanish.

The relevance of the procedure is put in light in Figure 8, where we can far more easily see the resonance frequencies of the tube in the sediment. A theoretical computation of the tube resonance frequencies gives 10 resonance values for the product $k_{sed} \cdot a$ between 10 and 40: 10.04, 13.13, 16.23, 19.33, 22.43, 25.51, 28.57, 31.61, 34.62 and 37.60, and most of them are clearly observable in Figure 8.

To compute the acoustic field scattered by the rigid cylinder near a plane interface, only two parameters are required: the radius a and the distance from the interface h. Because the GMI is a very tractable approach, we can compute this acoustic field for a lot of different a and h values. Eventually, applying a fitting process, the detection of the resonance frequencies related to an unknown elastic cylinder could be investigated.

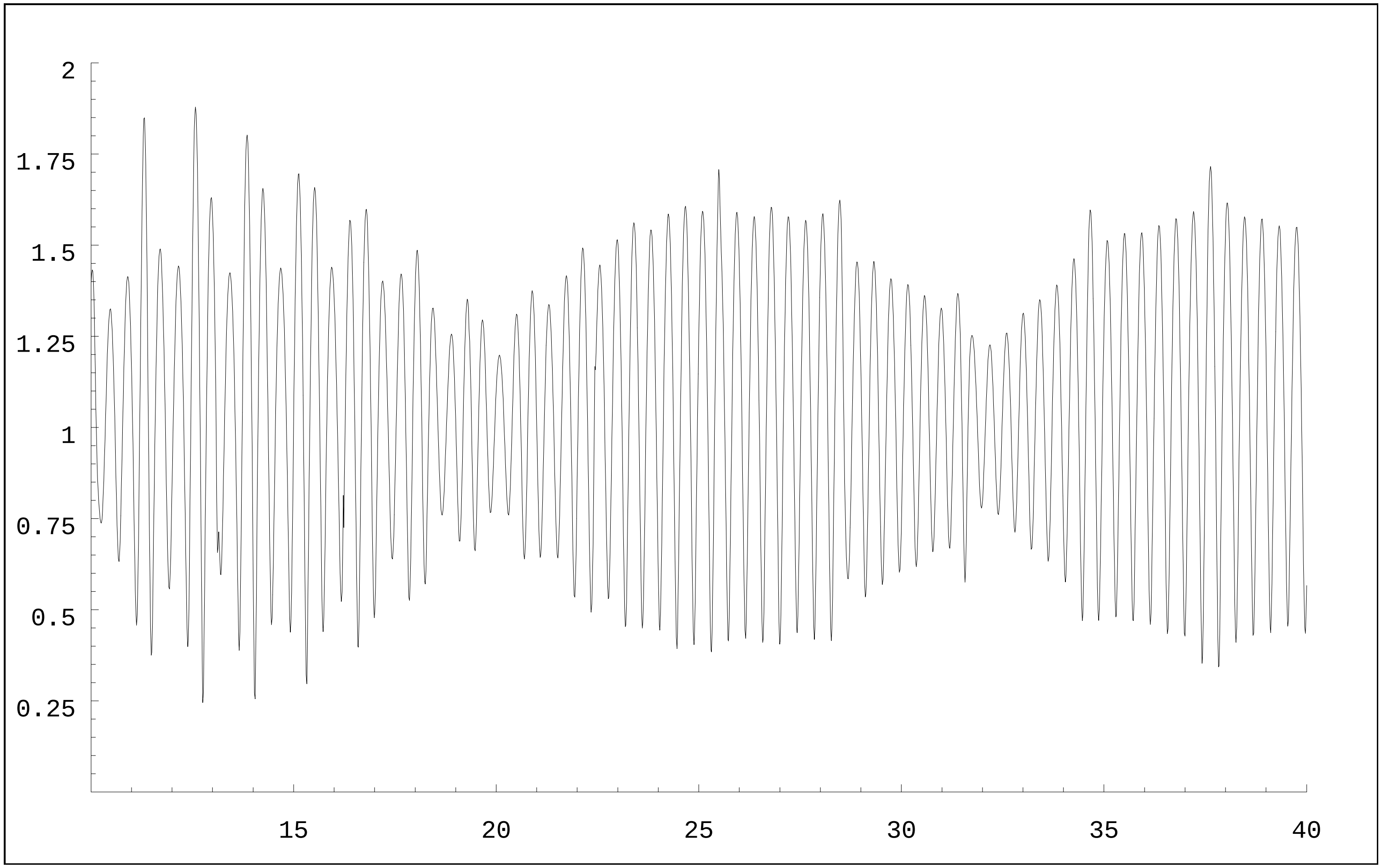

Fig. 7. *Scattering by an elastic tube embedded in a sediment.*

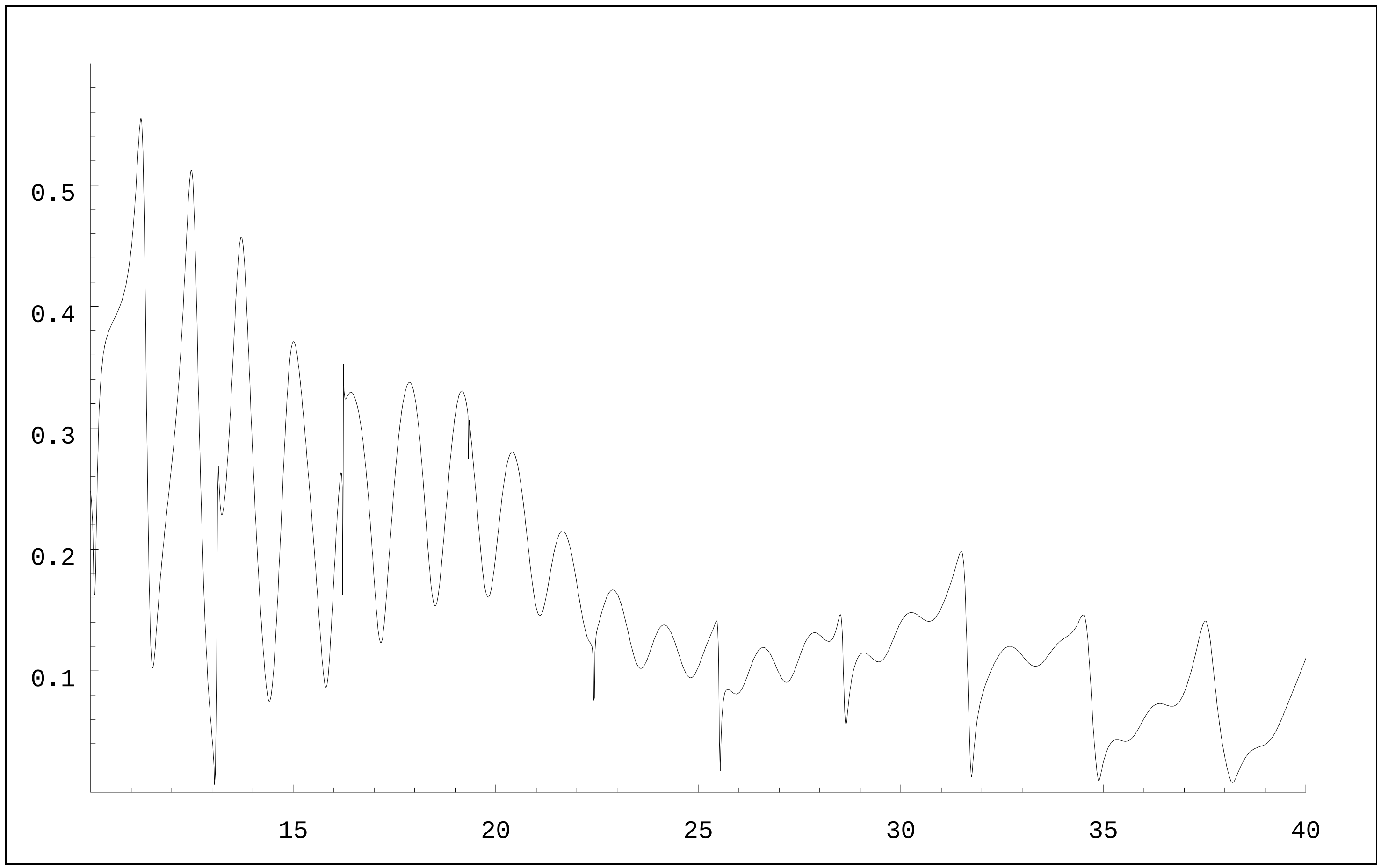

Fig. 8. *Scattering by an elastic tube embedded in the sediment minus the scattering by a rigid cylinder embedded in the same sediment received by an observer located in the surrounding fluid.*

4 Conclusion

First, this paper deals with a modal theory developed in order to estimate the scattering by an elastic cylinder embedded in a sediment. In the case of an observer located in the sediment, this theoretical description is mainly based on the generalization of the method of images (GMI). Approximating the sediment by a fluid medium, GMI leads to a robust and tractable method involving interferences between a cylinder and a penetrable plane interface close the one from the other. Furthermore, assuming the **T**-matrix (describing the cylinder scattering) as known [21], GMI is well adapted to every kind of cylinders with non-circular cross section, anisotropy and so on...

In the case of an observer located in the fluid above the sediment, an hypothesis of hight frequency has been introduced. So, combining the GMI with the calculation of integrals with the aid of the steepest descent approximation, a reliable evaluation of the acoustic field transmitted from the sediment to the fluid has been obtained.

Finally, we have shown that our approach yields a promising method to detect the elastic resonances of an elastic cylinder embedded in the sediment with a good tractability. Actually, we think our model could be usefully applied to the detection of elastic cylinders in sedimentary media.

References

[1] M. F. Werby, C. G. Gaunaurd, Resonance in the backscattered echoes from elastic shells near an interface, in: Elastic Wave Propagation, mccarthy and hayes Edition, Elsevier Science Publishers (North-Holland), 1989, pp. 393–398.

[2] C. G. Gaunaurd, Distortions in the backscattering cross-section of a submerged elastic target produced by its proximity to the sea surface bottom, in: Computational Acoustics, lee, cakmak and vichnevetsky Edition, Vol. 2, Elsevier Science Publishers (North-Holland), 1990, pp. 25–37.

[3] G. C. Gaunaurd, H. Huang, Acoustic scattering by a spherical body near a plane boundary, J. Acoust. Soc. Am. 96 (4) (1994) 2526–2536.

[4] H. Huang, G. C. Gaunaurd, Acoustic point source scattering by a spherical elastic shell submerged beneath a free surface, J. Acoust. Soc. Am. 99 (5) (1996) 2720–2726.

[5] V. Twersky, Multiple scattering of radiation by an arbitrary configuration of parallel cylinders, J. Acoust. Soc. Am. 24 (1) (1952) 42–46.

[6] V. Twersky, Multiple scattering of radiation by an arbitrary planar configuration of parallel cylinders and by two parallel cylinders, J. Appl. Phys. 23 (4) (1952) 407–414.

[7] J. A. Fawcett, A plane-wave decomposition method for modelling scattering from objects and bathymetry in a waveguide, J. Acoust. Soc. Am. 100 (1) (1996) 183–192.

[8] G. Taraldsen, The complex image method, Wave Motion 43 (1) (2006) 91–97.

[9] A. Coatanhay, J.-M. Conoir, Scattering near a plane interface using a generalized method of images approach, J. Comp. Acoust. 12 (2) (2004) 233–256.

[10] A. Coatanhay, J.-M. Conoir, Scattering by an elastic cylinder buried in a sedimentary fluid medium, in: 135th conference of American Society of Acoustic, Seattle (Wa), USA, 1998.

[11] P. M. Morse, H. Feshbach, Methods of Theoretical Physics, McGraw-Hill, New-York, 1968.

[12] D. E. Chimenti, A. H. Nayeh, D. L. Butler, Leaky rayleigh waves on a layered halfspace, J. Acoust. Soc. Am. 53 (1) (1982) 170–176.

[13] D. B. Bogy, S. M. Gracewski, Nonspecular reflection of bounded acoustic beams from the liquid-solid interface of two elastic layers on a halfspace under water, Int.J.Solids.Structures 20 (8) (1984) 747–760.

[14] A. H. Nayfeh, T. W. Taylor, Surface wave characteristics of fluid-loaded multilayered media, J. Acoust. Soc. Am. 84 (6) (1988) 2187–2191.

[15] L. M. Brekhovskikh, O. A. Godin, Acoustics of layered media I. Plane and quasi-plane waves, Vol. 5 of Springer series on wave phenomena, Springer-Verlag, Berlin, 1990.

[16] L. Tsang, J. A. Kong, K.-H. Ding, Scattering of electromagnetic waves. Theories and applications., Series in remote sensing, Wiley, 2000.

[17] J. J. Faran, Sound scattering by solid cylinders and spheres, J. Acoust. Soc. Am. 23 (1951) 405–418.

[18] R. D. Doolittle, H. Überall, P. Uginčius, Sound scattering by elastic cylinders, J. Acoust. Soc. Am. 43 (1968) 1–14.

[19] L. Flax, W. G. Neubauer, Acoustic reflection from layered elastic absorptive cylinders, J. Acoust. Soc. Am. 61 (1977) 307–312.

[20] N. D. Veksler, Resonance Acoustic Spectroscopy, Springer-Verlag, 1993.

[21] V. Varadan, Scattering matrix for elastic waves. II., J. Acoust. Soc. Am. 63 (4) (1978) 1014–1024.

[22] M. Abramowitz, I. Stegun, Handbook of mathematical functions, Dover Publications, New-York, 1965.

[23] A. Sommerfeld, Partial differential equations in physics, Academic Press, New-York, 1949.

[24] A. Coatanhay, Acoustic scattering by a cylindrical object in vicinity of a plane interface, Ph.D. thesis, Universit du Havre, in french (2000).

[25] J. A. Fawcett, Evaluation of the integrals of traget/seabed scattering using the method of complex images, J. Acoust. Soc. Am. 114 (3) (2003) 1406–1415.

[26] G. H. Hardy, Divergent series, Oxford University Press, New York, 1949.

[27] W. Balser, Formal Power Series and Linear Systems of Meromorphic Ordinary Differential Equations, Springer-Verlag, New-York, 2000.